Classification of hypervascular liver lesions based on hepatic artery and portal vein blood supply coefficients calculated from triphasic CT scans

F. Edward Boas, Aya Kamaya, Bao Do, Terry S. Desser, Christopher F. Beaulieu, Shreyas S. Vasanawala, Gloria L. Hwang, Daniel Y. Sze

Abstract

Perfusion CT of the liver typically involves scanning the liver at least 20 times, resulting in a large radiation dose. We developed and validated a simplified model of tumor blood supply that can be applied to standard triphasic scans, and evaluated whether this can be used to distinguish benign and malignant liver lesions. Triphasic CTs of 46 malignant and 32 benign liver lesions were analyzed. For each phase, regions of interest were drawn in the arterially enhancing portion of each lesion, as well as the background liver, aorta, and portal vein. Hepatic artery and portal vein blood supply coefficients for each lesion were then calculated by expressing the enhancement curve of the lesion as a linear combination of the enhancement curves of the aorta and portal vein. Hepatocellular carcinoma (HCC) and hypervascular metastases on average both had increased hepatic artery coefficients compared to the background liver. Compared to HCC, benign lesions on average had either a greater hepatic artery coefficient (hemangioma), or greater portal vein coefficient (focal nodular hyperplasia, or transient hepatic attenuation difference). Hypervascularity with washout is a key diagnostic criterion for HCC, but it had a sensitivity of 72% and specificity of 81% for diagnosing malignancy in our diverse set of liver lesions. The sensitivity for malignancy was increased to 89% by including enhancing lesions that were hypodense on all phases. The specificity for malignancy was increased to 97% (p=0.039) by also examining hepatic artery and portal vein blood supply coefficients, while maintaining a sensitivity of 76%.

Keywords: triphasic CT; enhancement; washout; hepatocellular carcinoma; liver lesions; computer-aided diagnosis

Abbreviations

AASLD American association for the study of liver diseases
EASL European association for the study of the liver
FNH focal nodular hyperplasia
HAC hepatic artery coefficient, or hepatic artery blood supply coefficient
HCC hepatocellular carcinoma
HU Hounsfield units
PVC portal vein coefficient, or portal vein blood supply coefficient
RFA radiofrequency ablation
ROI region of interest

TACE   transarterial chemoembolization
THAD   transient hepatic attenuation difference

1. Introduction

A variety of benign and malignant liver lesions can be characterized using contrast-enhanced CT. The optimal times for imaging the liver are during the late-arterial phase (35 second after contrast injection), when hypervascular liver lesions tend to have the greatest enhancement relative to background liver, the portal venous phase (60-70 seconds), when hypovascular liver metastases and the portal veins are best visualized, and the delayed (or equilibrium) phase (3-5 minutes), when washout or contrast retention can be best characterized. The non-enhanced phase provides minimal additional diagnostic information for liver lesions [1, 2], and to reduce the radiation dose, it is no longer part of our institution's multiphasic liver CT protocol.

On triphasic CT, hepatocellular carcinoma (HCC) is characteristically hyperdense compared to the surrounding liver in the arterial phase, iso- or hypo-dense compared to liver in the portal venous phase, and hypodense compared to liver in the delayed phase [1, 3]. Arterial phase enhancement (hyperdense compared to surrounding liver) with portal venous or delayed phase washout of contrast (hypodense compared to surrounding liver) [4] is considered diagnostic of HCC in cirrhotic livers, according to both EASL [5] and AASLD [6] guidelines.

However, not all hepatocellular carcinomas demonstrate contrast washout on delayed imaging, and not all lesions with washout are HCCs. A minority of well differentiated HCCs are hypodense to the liver on all phases [7]. Some hypervascular HCCs do not have washout [8]. Washout can also be seen in other liver lesions (both benign and malignant), including regenerative nodules [9], hemangiomas [10], focal nodular hyperplasia (FNH) [11], adenomas [12], and hypervascular metastases such as neuroendocrine tumors [13].

The appearance of the liver on various phases of imaging is thought to be related to the liver's dual blood supply. The normal liver receives about 70% of its blood flow from the portal vein, and 30% from the hepatic artery [14]. HCC receives most of its blood flow from the hepatic artery [15], which enhances and de-enhances before the portal vein does. Washout is presumably related to rapid displacement of highly enhanced blood with less enhanced blood in tissue that is predominantly supplied by the hepatic artery.

Liver perfusion CT typically involves scanning the liver at numerous (>20) time points after injection of IV contrast. The resulting enhancement curves can then be used to calculate blood volumes, blood flow, and capillary permeability [15, 16]. One goal of perfusion CT is to improve detection and characterization of liver lesions compared to standard triphasic imaging [16]. However, perfusion CT typically requires dedicated protocols and a large radiation dose, and the role of perfusion parameters in distinguishing benign and malignant liver lesions has not yet been established.

To address these limitations, we introduce the concept of the hepatic artery and portal vein blood supply coefficients (HAC and PVC), which provide a simple way to characterize enhancement curves quantitatively on standard triphasic CTs (arterial, portal venous, and delayed phases). We propose using the hepatic artery and portal vein coefficients to classify hypervascular liver lesions and to increase diagnostic accuracy by computer-aided diagnosis.

The HAC and PVC describe the enhancement curve of a liver lesion (which only contain 3 points in a triphasic scan) as a linear combination of the aortic and portal venous enhancement curves (Figure 1). For example, an enhancement curve that has the same shape as the aortic enhancement curve, but only half the amount of enhancement, is considered to have 50% HAC. An enhancement curve that is halfway between the enhancement curves of the aorta and portal vein is considered to have 50% HAC and 50% PVC. Thus, HAC indicates similarity of a lesion's enhancement curve to the aortic enhancement curve, and PVC indicates similarity of a lesion's enhancement curve to the portal venous enhancement curve.

The HAC and PVC are equal to hepatic artery and portal vein blood volumes, in a simple perfusion model that assumes rapid blood flow (no delay between enhancement of the supplying vessel and the tissue), and no vascular permeability to contrast (Figure 2). Blood volumes or coefficients are expressed in units of blood volume in a voxel (ml) divided by total volume of the voxel (ml), or as a percentage. Lesions with high HAC will show washout, compared to background liver, which has high PVC. Delayed enhancement (green line in Figure 1) cannot be explained by a model that assumes rapid flow and no leakage of contrast from vessels. However, since the enhancement increases in the delayed phase, whereas both the aorta and portal vein have decreased enhancement in the delayed phase, the green line has a negative calculated HAC and PVC. In the case of delayed enhancement, the calculated HAC and PVC describe the shape of the enhancement curve, but do not correspond to actual blood volumes.

In this paper, we examine whether hepatic artery and portal vein coefficients calculated from standard triphasic CTs can be used to distinguish benign and malignant liver lesions.
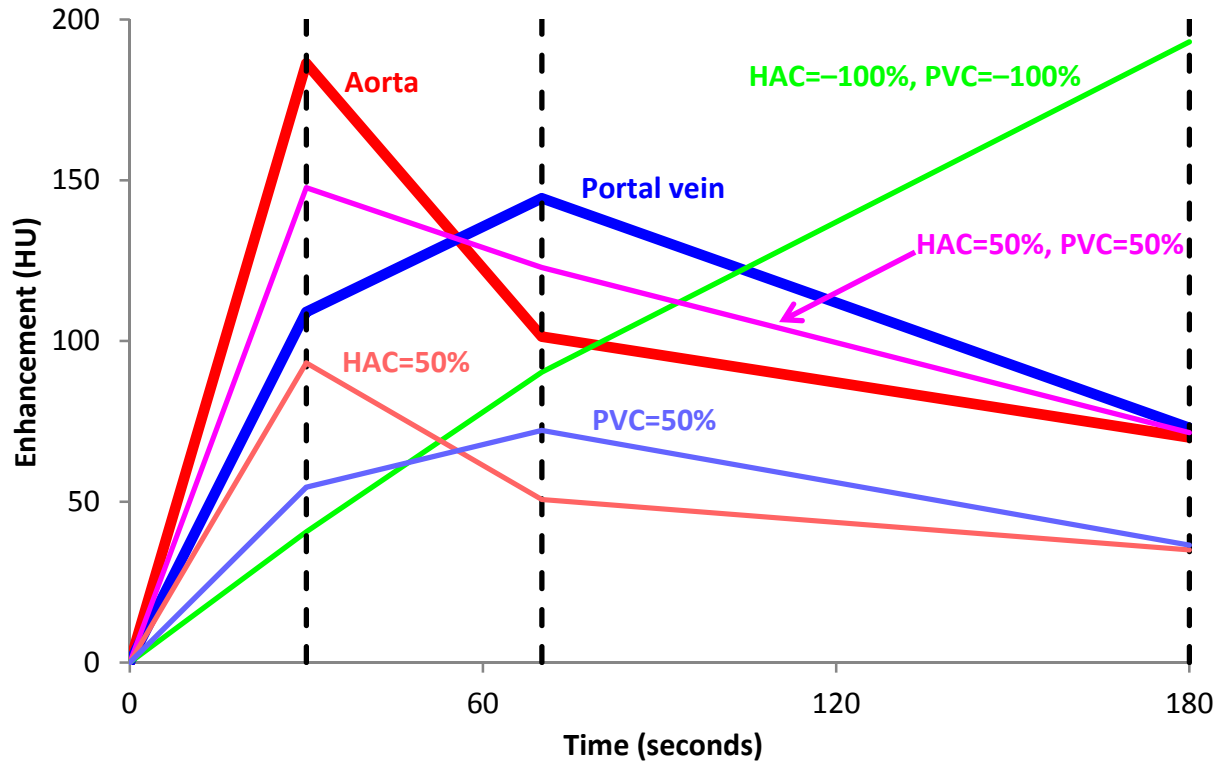
Figure 1. Schematic diagram of hepatic artery and portal vein coefficients calculated from a triphasic CT. The enhancement curve of a tumor or surrounding liver is expressed as a linear combination of the aortic and portal venous enhancement curves. The three phases in the triphasic scan are indicated by vertical dashed lines. The measured enhancement curves of the aorta and portal vein are plotted using thick lines. Other enhancement curves (thin lines) are labeled with their calculated coefficients.
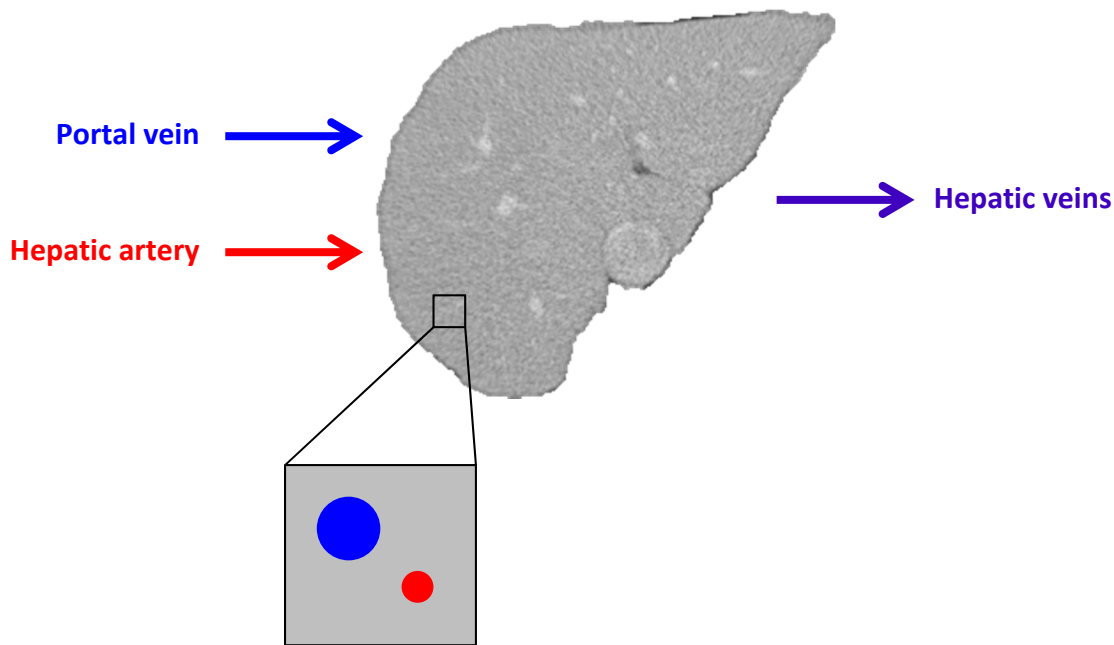
Figure 2. Simple model of liver perfusion. Branches of the portal vein are assumed to have the same enhancement curve as the main portal vein. Branches of the hepatic artery are assumed to have the same enhancement curve as the aorta. The enhancement of the liver parenchyma is due to small vessels that are below the resolution of CT. Normal liver parenchyma contains both portal vein and hepatic artery branches, so the enhancement will be a linear combination of the portal vein and hepatic artery enhancement curves. A hypervascular tumor will contain a greater proportion of hepatic artery branches, and the enhancement curve will more closely follow the hepatic artery enhancement curve.

2. Materials and methods

2.1. Patient selection and scan parameters

The institutional review board approved this retrospective HIPAA-compliant study; informed patient consent was waived. A diverse set of liver lesions with pre-treatment triphasic CT scans was obtained by searching for diagnoses that can be hypervascular. A database of radiology reports (impression section only) was searched for the following terms: focal nodular hyperplasia, transient hepatic attenuation difference, arterioportal shunt, adenoma, hypervascular metastasis, hemangioma, and regenerative nodule. In addition, a database search was performed to identify hepatocellular carcinomas that were treated by resection, transplant, transarterial chemoembolization (TACE), or radiofrequency ablation (RFA). The two largest lesions on the pre-treatment scan were examined.

Typical scan parameters were as follows: 120-150 mL of iodinated contrast (iopamidol 300 – 370 mg iodine/ml) was power injected intravenously at a rate of 4–5 ml/s. The liver was imaged at 30-35 s (arterial phase), 60-70 s (portal venous phase), and 180 s (delayed phase) after the start of contrast injection, using a kVp of 100 – 120 [4]. The following scanners were used: Siemens Definition, Siemens Definition AS+, Siemens SOMATOM Definition, Siemens Sensation 64, GE Discovery CT750 HD, GE LightSpeed 16, and GE LightSpeed VCT. Images were reconstructed using a soft tissue kernel, with a slice thickness between 1 and 5 mm.

For each diagnosis, cases with pre-treatment triphasic CT scans were evaluated for inclusion in the study (Table 1). Cases were excluded if the arterially enhancing portion of the lesion was too small to characterize ($\leq$ 5 mm), or if the main portal vein was completely occluded. In addition, cases were excluded if the peak enhancement of the aorta was not during the arterial phase, or the peak enhancement of the portal vein was not during the portal venous phase. This eliminated cases where the aorta and portal vein had similar enhancement curves (due to a poor bolus, or mis-timed scan), which would make it difficult to calculate accurate coefficients.

The diagnosis was based on the radiology reports (including MRI and follow up studies), and pathology (if available). Many of the lesions did not have pathologic confirmation. This allowed us to analyze lesions with classic imaging features that are not biopsied, as well as borderline lesions that are followed by imaging, but never biopsied. Regenerative nodules that did not have pathologic confirmation had to meet all of the following criteria: resolution on followup imaging or stability for at least 250 days, normal AFP, and no suspicious features on MRI (if available). Evaluation for cirrhosis was based on pathology (if available), or based on the CT appearance of the liver.

The study group included 78 liver lesions in 64 patients (Table 1). There were 40 HCCs, 10 regenerative nodules, 9 transient hepatic attenuation differences (THADs) [17], 7 hemangiomas, 6 hypervascular metastases, 4 FNHs, and 2 adenomas. The THADs were secondary to alterations in blood flow from portal vein occlusion (2 cases), hemangioma (1 case), abscess (1 case), around the falciform ligament (1 case), and unknown (4 cases).

Diagnosis	Initial number of lesions	Number of excluded lesions	Final number of lesions	Path. proven	Cirrhotic
HCC (explant or resection)	20	1 *, 1 ‡	18	100%	44%
HCC (RFA)	7	0	7	71%	100%
HCC (TACE)	15	0	15	27%	93%
Hypervascular metastasis	13	6 *, 1 †	6	67%	17%
Regenerative nodule	11	1 †	10	10%	70% §
FNH	6	2 *	4	50%	0%
THAD	10	1 *	9	0%	22%
Hemangioma	17	6 *, 4 †	7	0%	0%
Adenoma	2	0	2	50%	0%
Total / Average	101	23	78	45%	50%

Table 1. Liver lesions examined in this study.
* Peak enhancement of the aorta was not during the arterial phase, or peak enhancement of the portal vein was not during the portal venous phase.
† Enhancing portion of the lesion was too small to characterize (≤ 5 mm).
‡ Complete occlusion of the main portal vein.
§ Non-cirrhotic cases had Budd Chiari syndrome.

2.2. Calculation of hepatic artery and portal vein blood supply coefficients

Hepatic artery and portal vein coefficients were calculated from the pretreatment triphasic CT (arterial, portal venous, and delayed phases). The three phases were manually aligned by translation in the *x*, *y*, and *z* directions. For each phase, regions of interest (ROIs) were drawn over the liver, aorta (at the level of the celiac artery), and portal vein (near the bifurcation). For heterogeneous lesions, measurements were made in the most arterially enhancing portion of the lesion, and in the same location on the other phases. ROIs were elliptical, with a length of at least 5 mm. ROIs were also drawn over the background liver. Large intrahepatic vessels were avoided when drawing the ROIs in the liver. The liver enhancement curves were expressed as a linear combination of the hepatic artery and portal venous enhancement curves. Specifically, for each pixel in the liver:

$$x_i = \mathrm{HAC} \cdot a_i + \mathrm{PVC} \cdot v_i \,,$$

where x_i is the enhancement of the pixel in the liver, a_i is the enhancement of the aorta, and v_i is the enhancement of the portal vein. $i=1$ is the arterial phase, $i=2$ is the portal venous phase, and $i=3$ is the delayed phase. Enhancement was measured in Hounsfield units, relative to the

average Hounsfield units of the three phases (we typically do not obtain non-contrast images). Thus:

$$x_1 + x_2 + x_3 = 0 \,,$$
$$a_1 + a_2 + a_3 = 0 \,, \text{ and}$$
$$v_1 + v_2 + v_3 = 0 \,.$$

Solving these equations for HAC and PVC yields:

$$\mathrm{HAC} = (v_2 x_1 + v_2 x_2 + v_3 x_2)/(a_2 v_3 - a_3 v_2)$$
$$\mathrm{PVC} = (a_2 x_1 + a_2 x_2 + a_3 x_2)/(a_3 v_2 - a_2 v_3)$$

Calculated HAC and PVC for each pixel in the liver were then displayed on both grayscale and color images (Figure 3 and Appendix). The three color channels in the color image summarize the information from the three post-contrast images. Color images were generated using a custom web application written in PHP, Javascript, and C++.

Enhancement
None———————►Intense

Aortic phase
Portal venous phase
Delayed phase
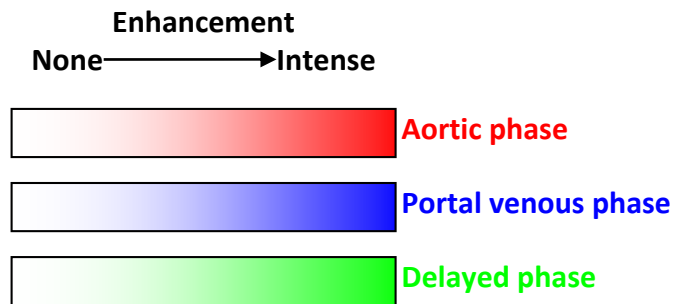
Figure 3. Color scale for the images in Figure 6. The color indicates the phase of enhancement (based on the HAC and PVC). The saturation (grayscale versus color) indicates the degree of enhancement. The brightness is related to the average Hounsfield units over the three phases (not shown).

2.3. Model validation

7 consecutive triphasic liver scans that showed no focal liver lesions, and had clearly visualized hepatic veins were evaluated. For each scan, the HAC and PVC of the liver parenchyma was used to calculate the expected enhancement curve of the right hepatic vein:

Predicted hepatic vein enhancement = $x_i/(\mathrm{HAC} + \mathrm{PVC})$.

This prediction made by our simple model of liver perfusion was then compared to the measured enhancement.

2.4. Lesion classification and statistical analysis

Relative enhancement pattern (density of the most arterially enhancing portion of the lesion compared to the surrounding liver) was based on average Hounsfield unit measurements in the

lesion, compared to the surrounding liver, calculated from manually drawn ROIs. Lesions were characterized as hyperdense, isodense, or hypodense relative to surrounding liver in the arterial and delayed phases. For example, "hypervascular with washout" indicates that portions of the lesion are hyperdense relative to the background liver on the arterial phase, and those portions become hypodense relative to the surrounding liver on the delayed phase. Lesions were classified as malignant if > y% of lesions with the same relative enhancement pattern were malignant; the sensitivity and specificity of the classification were examined for different values of y [18]. In other words, if a given relative enhancement pattern is always associated with malignant lesions, then that relative enhancement pattern should be considered malignant. If a given relative enhancement pattern is associated with both benign and malignant lesions, then that relative enhancement pattern could be considered either benign or malignant, depending on the value of y, which is adjusted to achieve the desired sensitivity and specificity.

Lesions were also classified as malignant if their hepatic artery and portal vein coefficients fell within ranges that were similar to other malignant lesions (2D linear classifier). The ranges were chosen to maximize the sum of the sensitivity and specificity [19], using a hill climbing optimization algorithm.

Sensitivity and specificity were calculated on a per-lesion basis. Statistical comparisons were performed using a two-tail, two-sample t-test assuming unequal variances. Confidence intervals of proportions were calculated assuming a uniform prior distribution [20]. Differences between proportions were evaluated using a two-tail z-test.

3. Results

3.1. Model validation

Figure 4 shows good agreement between predicted and measured hepatic vein enhancement. Although predicting hepatic vein enhancement does not have clinical significance, the agreement between the prediction and reality provides some support for our simple model of liver perfusion.
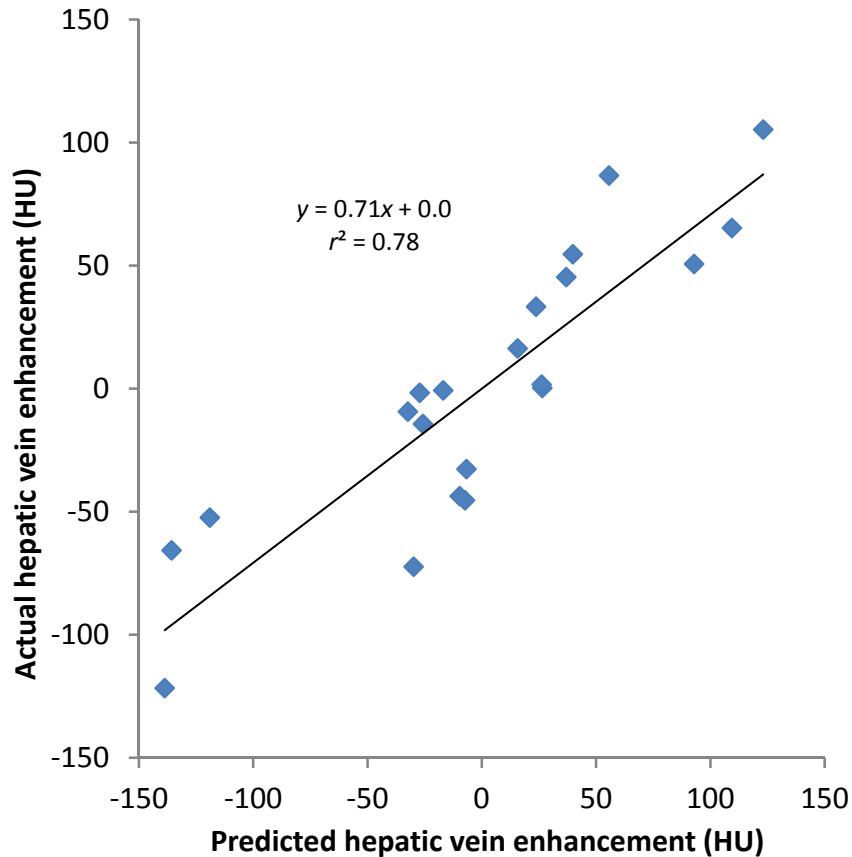
Figure 4. Predicted versus measured enhancement of the right hepatic vein (Hounsfield units, relative to the average of the three phases). Each point represents a single phase of a single triphasic CT. The predicted enhancement of the hepatic vein is based on the enhancement of the aorta, portal vein, and liver parenchyma.

3.2. Hepatic artery and portal vein coefficients

Hepatic artery and portal vein coefficients of non-cirrhotic liver, cirrhotic liver, as well as various liver lesions are shown in Figure 5 and Table 2. There was significant overlap between different liver lesions. However, malignant lesions tended to have perfusion characteristics that fell within the grey rectangle, while benign lesions had a wider range of perfusion characteristics, and mostly fell outside the gray rectangle. Classification of liver lesions on the basis of perfusion characteristics is described in the next section.

Cirrhotic liver had decreased portal vein coefficient (PVC) compared to normal liver ($p=2.4\times10^{-8}$). HCC had increased hepatic artery coefficient (HAC) compared to the background liver ($p=8.8\times10^{-17}$). Hypervascular metastases had similar HAC and PVC compared to HCCs. Hemangioma had increased HAC compared to HCC.

FNH and THAD both had increased PVC compared to HCC. Two of the THADs were caused by occlusion of a branch of the portal vein. In both cases, both the hepatic artery and portal vein coefficients were increased compared to portions of the liver supplied by a patent portal vein.

Regenerative nodules had a wide range of hepatic artery and portal vein coefficients, but the average coefficients were not statistically significantly different from HCC. Some regenerative nodules had increased PVC compared to HCC, like THADs. Others had characteristics that overlapped with cirrhotic liver. One nodule had increased HAC compared to HCC, like a hemangioma.

Hepatic artery and portal vein coefficients can be displayed on grayscale or color images (Figure 3 and Figure 6). Each type of lesion had a characteristic appearance on color images. Notice that the aorta is bright red and the portal vein is bright blue. Normal liver is light blue, indicating that the enhancement curve follows the portal vein, but is not as intense. Hypervascular liver lesions are typically purple, indicating that the shape of the enhancement curve is in between that of the aorta and portal vein. Fat and muscle are gray, indicating minimal enhancement. The artifactual color near edges is due to misalignment among the three phases.

Diagnosis	n	HAC average	st. dev.	PVC average	st. dev.
HCC	40	10%	11%	23%	17%
Hypervascular metastasis	6	24%	14%	30%	11%
Regenerative nodule	10	6%	22%	34%	20%
FNH	4	23%	10%	43% *	7%
THAD	9	12%	14%	47% *	18%
Hemangioma	7	64% *	23%	33%	29%
Adenoma	2	33% *	2%	45% *	1%
Non-cirrhotic liver †	36	-12%	7%	52%	14%
Cirrhotic liver †	38	-13%	7%	31%	14%

Table 2. Hepatic artery coefficients (HAC) and portal vein coefficients (PVC) for various liver lesions (untreated), in ml/ml (%).
* Statistically significant difference compared to HCC. To correct for multiple comparisons, a cutoff p value of 0.05 / 12 = 0.0042 was used to determine statistical significance.
† Excluding liver transplants and Budd-Chiari. If lesions in both the right and left liver were analyzed, then ROIs were drawn in both the right and left lobes of the liver.
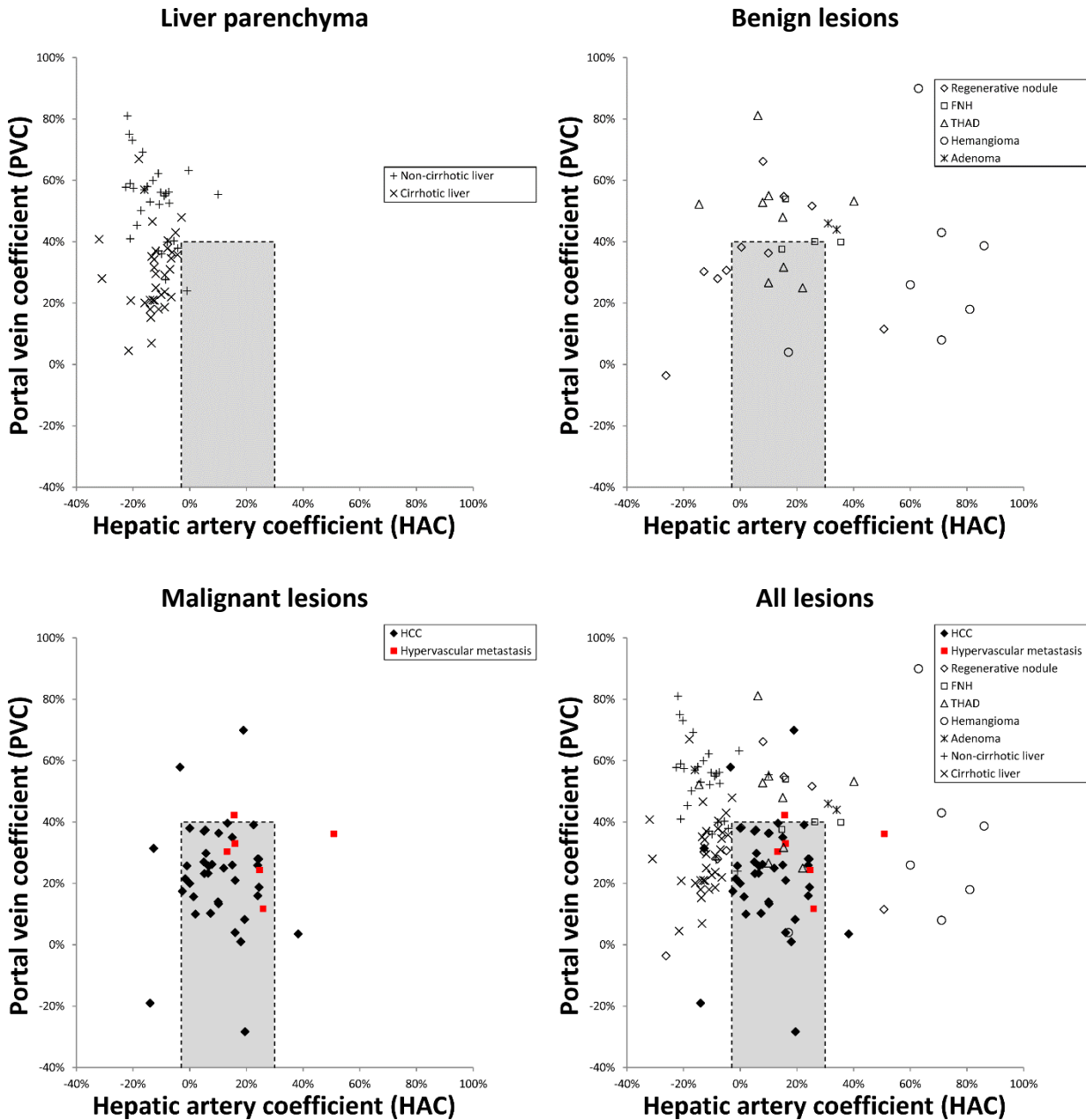
Figure 5. Hepatic artery and portal vein coefficients for untreated liver lesions, coded by diagnosis. Malignant lesions are shown as solid filled shapes, and benign lesions are shown as open shapes. Lesions in the gray rectangle were classified as malignant. The size and position of the grey rectangle were chosen to maximize the sum of the sensitivity and specificity of the classification.
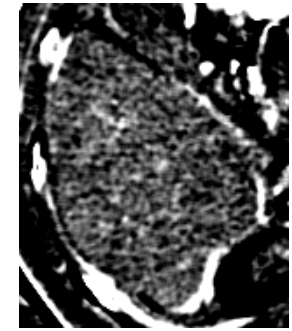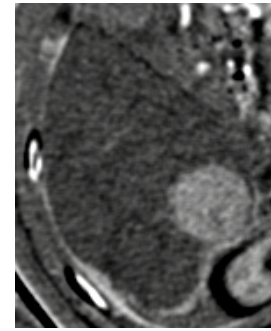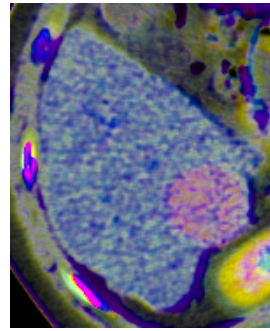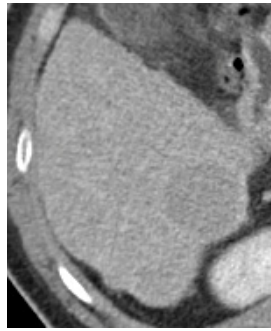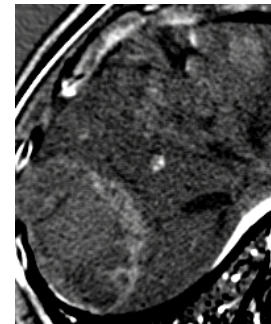
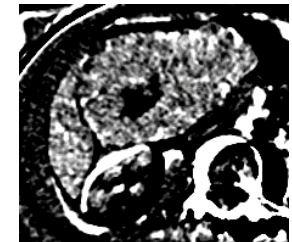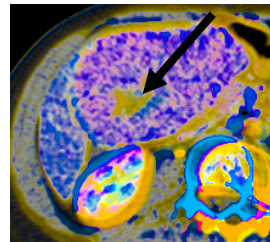| Diagnosis	Arterial phase	Delayed phase	Color image	Hepatic artery coeff.	Portal vein coefficient
HCC					
Metastases					
FNH					
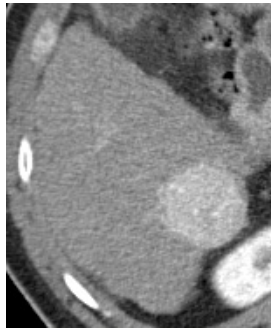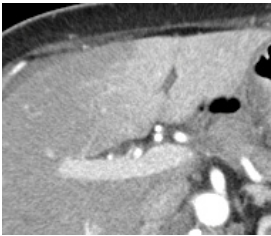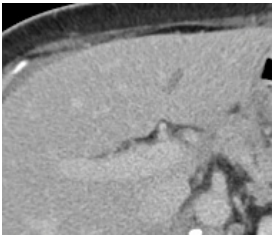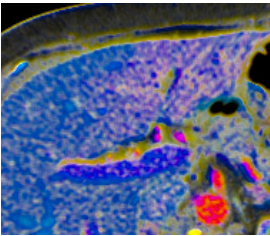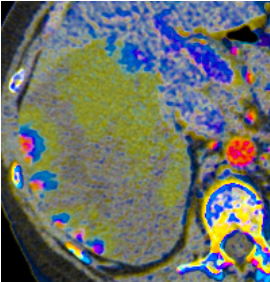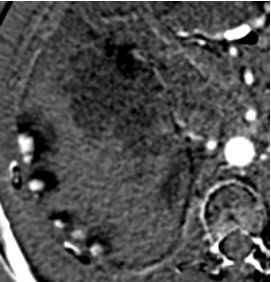
Diagnosis	Arterial phase	Delayed phase	Color image	Hepatic artery coeff.	Portal vein coefficient
THAD					
Hemangioma					

Figure 6. Hepatic artery and portal vein coefficients, calculated from triphasic scans. The images in each column are displayed at the same window/level settings. The color scale is shown in Figure 3. The full 3D datasets are available as an interactive figure at http://www.claripacs.com/a.php?a=5q

Top row: Moderately differentiated HCC (pathology proven). The pink color of the lesion indicates predominantly arterial inflow.

2nd row: Neuroendocrine tumor metastases to the liver (pathology proven).

3rd row: Focal nodular hyperplasia. Delayed enhancement of the central scar is shown in green (arrow) on the color image. The apparent washout of the lesion in the delayed phase is an optical illusion due to the enhancing rim [21]. Hounsfield unit measurements show that the lesion is isodense to liver on the delayed phase.

4th row: THAD surrounding the falciform ligament, which is a common location [17].

Last row: Giant hemangioma. Notice the peripheral foci of arterial phase enhancement (red), with enhancement progressing more centrally on later phases (blue and green).

3.3. Classification of liver lesions

In this diverse set of liver lesions, the most suspicious relative enhancement pattern was hypervascularity with washout (Table 3), which was seen in HCC, hypervascular metastases, and some benign lesions. The second most suspicious relative enhancement pattern was hypodensity on all phases, which was seen in HCC and regenerative nodules. (Hepatic cysts were not included in this study.) Using only the most suspicious relative enhancement pattern (hypervascularity with washout) to diagnose malignant lesions resulted in a sensitivity of 72% and specificity of 81%. Using the top two most suspicious relative enhancement patterns (hypervascularity with washout or hypodensity on all phases) to diagnose malignancy resulted in a sensitivity of 89% and specificity of 72%. (The improved sensitivity was statistically significant, but the decreased specificity was not.)

Liver lesions were also classified based on the hepatic artery and portal vein coefficients. As described above, HCC and hypervascular metastases had similar coefficients, while benign lesions had either greater portal vein coefficients (FNH or THAD), or greater hepatic artery coefficients (hemangioma). We therefore classified a lesion as malignant if the coefficients were similar to other malignant lesions. The optimal ranges for diagnosing malignancy were: HAC > −3%, HAC < 30%, and PVC < 40% (Figure 5). The resulting sensitivity was 85% and specificity was 78%. This was not statistically significantly different from using hypervascularity with washout to diagnose malignancy.

Requiring that a lesion be suspicious by both relative enhancement criteria (hypervascular with washout, or hypodense on all phases) and hepatic artery and portal vein coefficient criteria to be diagnosed as malignant resulted in a sensitivity of 76%, and a specificity of 97% (Table 4). This was a statistically significant improvement in specificity for detecting malignant liver lesions (p=0.039), compared to hypervascularity with washout.

Relative enhancement	n	% malignant (95% confidence interval)	Diagnoses
hypervascular with washout	39	85% (71–94%)	HCC (27; 6 well diff, 5 mod diff, 1 poorly diff, 15 unknown diff) metastasis (6) hemangioma (3) adenoma (2) regenerative nodule (1)
hypervascular on arterial phase, and isodense on the delayed phase	18	28% (11–50%)	THAD (6) HCC (5; 2 mod diff, 3 unknown diff) Regenerative nodule (3) FNH (4)
hypodense on all phases	11	73% (45–92%)	HCC (8; 3 well diff, 2 mod diff, 3 unknown diff) Regenerative nodule (3)
hyperdense on all phases	8	0% (0–28%)	Hemangioma (4) THAD (3) Regenerative nodule (1)
Other	2	0% (0–63%)	Regenerative nodule (2)

Table 3. Diagnosis by relative enhancement pattern.

Criterion	Sensitivity	Specificity
A. Hypervascular with washout	72%	81%
B. Hypervascular with washout, or hypodense on all phases	89% *	72%
C. HAC > −3%, HAC < 30%, and PVC < 40%	85%	78%
D. A and C	65%	97% *
E. B and C	76%	97% *

Table 4. Sensitivity and specificity for diagnosing malignant liver lesions (on a per-lesion basis). * indicates a statistically significant difference compared to hypervascularity with washout (criterion A).

4. Discussion

The clinical promise of CT perfusion imaging of the liver has largely been unfulfilled, for two major reasons: the increased radiation dose, and unclear clinical benefit. In our paper, we address both of these issues. We developed a simplified model of tumor blood supply that can be applied to standard triphasic scans, thus reducing the radiation dose relative to traditional perfusion imaging. We then show that blood volumes estimated from triphasic scans improve the specificity for diagnosing malignancy, compared to traditional criteria such as washout. Improved specificity may be especially helpful in non-cirrhotic livers, where imaging findings are currently considered insufficient for diagnosis of HCC, and biopsy is recommended [5, 6]. To our knowledge, this is the first time that liver perfusion parameters have been used to distinguish benign and malignant liver lesions.

Hepatic artery and portal vein coefficients provide an estimate of the blood volumes in liver lesions. The model of liver perfusion used to calculate these coefficients assumes that enhancement of the liver parenchyma is due to enhancement of small branches of the hepatic artery and portal vein, which follow the enhancement of the aorta and main portal vein, respectively. This assumption is reasonable, given that the liver transit time (approximately 10 seconds [22]) is less than the contrast bolus length (approximately 30 seconds). Furthermore, the model was validated by using it to predict the enhancement curves of the hepatic veins.

The model captures important aspects of liver physiology. As expected, cirrhosis decreases the portal vein coefficient, which corresponds to the reduced portal flow associated with cirrhosis. Portal vein occlusion results in increased HAC and PVC in the affected portion of the liver. We can speculate that this is analogous to the compensatory increased cerebral blood volume caused by vasodilation in an acute ischemic stroke [23].

Hepatic artery and portal vein coefficients calculated from pre-treatment triphasic CT scans can be used to classify hypervascular liver lesions. HCC and hypervascular metastases on average both had increased hepatic artery coefficients compared to the background liver, in agreement with prior results [15]. Compared to HCC, benign lesions on average had either greater portal vein coefficients (FNH or THAD), or greater hepatic artery coefficients (hemangioma).

The elevated blood volumes in hemangiomas corresponds to the increased blood volume seen on tagged red blood cell scans [24].

Regenerative nodules showed 3 different types of hepatic artery and portal vein coefficients, which were similar to cirrhotic liver, THADs, and hemangiomas. The clinical significance of these three different classes of coefficients is unclear, but it is possible that some of the lesions that are being diagnosed as "regenerative nodules" based on imaging, are actually THADs or hemangiomas.

Hepatic artery and portal vein coefficients improve the specificity for diagnosing malignancy in liver lesions, when combined with traditional relative enhancement criteria (such as washout).

Hypervascularity with washout is a key diagnostic criterion for HCC, but had a sensitivity of only 72% and specificity of 81% for diagnosing malignancy in a diverse set of liver lesions. Using the hepatic artery and portal vein blood supply coefficients, in addition to the relative enhancement patterns, computer-aided diagnosis resulted in a sensitivity of 76% and specificity of 97% for malignancy.

Thus, relative enhancement criteria (such as washout) and hepatic artery and portal vein coefficients provide complementary information about liver lesions. Washout considers the enhancement of both the lesion as well as the surrounding liver, whereas the HAC and PVC consider only the enhancement of the lesion itself. It would be interesting to examine HAC and PVC relative to the surrounding liver, but these would be technically challenging to measure accurately, because subtracting noisy coefficients would double the variance (assuming uncorrelated noise).

We developed an online calculator for liver lesion classification based on relative enhancement, HAC, and PVC: http://www.claripacs.com/calc/liver.html (Figure 7). Note that this classifier should not be applied to cysts, hypovascular metastases, or cholangiocarcinoma, which were not included in the training set.

The color images in Figure 6 summarize the information in the three phases of the scan, potentially allowing for a quicker assessment of multiple time points. Each type of liver lesion had a characteristic appearance on the color and grayscale images showing HAC and PVC. These color images encode three numbers per pixel (HAC, PVC, and average Hounsfield units), and thus have a higher information content than prior methods for colorizing multiphasic scans, which encode a single number per pixel [25]. The role of these color images in lesion detection or characterization should be examined in future studies.

There are several limitations to this study. First, the study population was selected to include a diverse set of liver lesions. The frequency of different types of lesions may be different in a different population, which could change the sensitivity, specificity, and pre-test probability. For example, the pre-test probability of HCC is higher in a cirrhotic liver (resulting in the recommendation that imaging alone can only be used to diagnose HCC in cirrhotic livers [5]). In this paper, we included both cirrhotic and non-cirrhotic livers. Second, we only examined lesion characterization, and not lesion detection, which will result in an overestimation of the sensitivity.

A third limitation is that we only examined HAC, PVC, and relative enhancement characteristics. Several other imaging features can be used to distinguish HCC from other liver lesions: portal vein invasion, abnormal internal vessels [3, 26], heterogeneous enhancement [3], large size [7], hyperintensity on T2 MRI sequences, and a pseudocapsule with delayed enhancement [27] all favor a diagnosis of HCC. Our findings should be confirmed with a prospective study, where the HAC and PVC are considered in the context of all of the other imaging and clinical data.

A fourth limitation is that the hepatic artery and portal vein coefficients are only equal to the hepatic artery and portal vein blood volumes if there is rapid blood flow and no leakage of contrast from the vessel. These assumptions are not valid when there is delayed enhancement. Delayed enhancement results in calculated blood volumes less than zero, which are not physiologic. Accurate blood volumes are difficult to obtain from the limited information in a triphasic scan. However, our estimated blood volumes were useful for classifying liver lesions, even if they do not quantitatively match the actual blood volumes. A more sophisticated model would require more contrast phases, and likely a higher radiation dose. However, a previous study showed that even with 60 time points, the enhancement curves only had sufficient information to fit a 3 parameter model, and a 5 parameter model was underdetermined [28]. In this paper, we had 3 time points, and used a 2 parameter model (HVC and PVC). Given the limited information in the enhancement curves, liver perfusion models all make a variety of different assumptions, and do not quantitatively match experimental measurements [16, 28].

Finally, the liver deforms with breathing, making it difficult to align exactly across phases. We aligned the phases using translation in three dimensions, but more sophisticated non-rigid alignment algorithms are available [25]. Furthermore, in heterogeneous lesions, we measured the most arterially enhancing portion of the lesion, but the exact choice of ROI is still somewhat arbitrary. Both of these factors introduce uncertainty into the calculated coefficients.

Conclusion

Hepatic artery and portal vein blood supply coefficients calculated from triphasic liver CT examinations can be used to classify hypervascular liver lesions. These coefficients improve the specificity for diagnosing malignancy in liver lesions, when combined with traditional relative enhancement criteria (such as washout).

Figure 7. Online liver lesion classification. See http://www.claripacs.com/calc/liver.html

Appendix

The red, green, and blue values for each pixel in the color images (ranging from 0 to 1) were calculated from the HAC, PVC, and Hounsfield units (averaged over the arterial, portal venous, and delayed phases), using the following pseudocode. The result is the color scale shown in Figure 3.

```
// the square root (sqrt) was added empirically to reduce color saturation.
// force_range(x,a,b) equals a if x<a, b if x>b, and x otherwise.
red = sqrt(force_range(1+HAC-PVC, 0, 2));
blue = sqrt(force_range(1-HAC+PVC, 0, 2));
green = sqrt(force_range(1-HAC-PVC, 0, 2));
// scale is used to make the brightness related to the Hounsfield units
if (max(red,green,blue) == 0)
  scale = 0;
else
  scale = force_range((HU-window_level+window_width/2)/window_width, 0,
1)/max(red,green,blue);
red=force_range(red*scale, 0, 1);
blue=force_range(blue*scale, 0, 1);
green=force_range(green*scale, 0, 1);
```

References

1.   Iannaccone R, et al.: Hepatocellular carcinoma: role of unenhanced and delayed phase multi-detector row helical CT in patients with cirrhosis. Radiology 234:460-467, 2005
2.   Doyle DJ, O'Malley ME, Jang HJ, Jhaveri K: Value of the unenhanced phase for detection of hepatocellular carcinomas 3 cm or less when performing multiphase computed tomography in patients with cirrhosis. J Comput Assist Tomogr 31:86-92, 2007
3.   Lee KH, O'Malley ME, Haider MA, Hanbidge A: Triple-phase MDCT of hepatocellular carcinoma. AJR Am J Roentgenol 182:643-649, 2004
4.   Liu YI, Shin LK, Jeffrey RB, Kamaya A: Quantitatively defining washout in hepatocellular carcinoma. AJR Am J Roentgenol 200:84-89, 2013
5.   Llovet JM, Ducreux M: EASL-EORTC clinical practice guidelines: Management of hepatocellular carcinoma. J Hepatol 56:908-943, 2012
6.   Bruix J, Sherman M: Management of hepatocellular carcinoma: an update. Hepatology 53:1020-1022, 2011
7.   Bolondi L, et al.: Characterization of small nodules in cirrhosis by assessment of vascularity: the problem of hypovascular hepatocellular carcinoma. Hepatology 42:27-34, 2005
8.   Kim SH, et al.: Gadoxetic acid-enhanced MRI versus triple-phase MDCT for the preoperative detection of hepatocellular carcinoma. AJR Am J Roentgenol 192:1675-1681, 2009
9.   Brancatelli G, Baron RL, Peterson MS, Marsh W: Helical CT screening for hepatocellular carcinoma in patients with cirrhosis: frequency and causes of false-positive interpretation. AJR Am J Roentgenol 180:1007-1014, 2003
10.   Freeny PC, Marks WM: Hepatic hemangioma: dynamic bolus CT. AJR Am J Roentgenol 147:711-719, 1986
11.   Carlson SK, Johnson CD, Bender CE, Welch TJ: CT of focal nodular hyperplasia of the liver. AJR Am J Roentgenol 174:705-712, 2000
12.   Ichikawa T, Federle MP, Grazioli L, Nalesnik M: Hepatocellular adenoma: multiphasic CT and histopathologic findings in 25 patients. Radiology 214:861-868, 2000
13.   Sica GT, Ji H, Ros PR: CT and MR imaging of hepatic metastases. AJR Am J Roentgenol 174:691-698, 2000
14.   Schenk WG, Jr., Mc DJ, Mc DK, Drapanas T: Direct measurement of hepatic blood flow in surgical patients: with related observations on hepatic flow dynamics in experimental animals. Ann Surg 156:463-471, 1962
15.   Li JP, et al.: Assessment of tumor vascularization with functional computed tomography perfusion imaging in patients with cirrhotic liver disease. Hepatobiliary Pancreat Dis Int 10:43-49, 2011
16.   Pandharipande PV, Krinsky GA, Rusinek H, Lee VS: Perfusion imaging of the liver: current challenges and future goals. Radiology 234:661-673, 2005
17.   Desser TS: Understanding transient hepatic attenuation differences. Semin Ultrasound CT MR 30:408-417, 2009
18.   Obuchowski NA: Receiver operating characteristic curves and their use in radiology. Radiology 229:3-8, 2003

19.   Kaivanto K: Maximization of the sum of sensitivity and specificity as a diagnostic cutpoint criterion. J Clin Epidemiol 61:517-518, 2008

20.   Boas FE: Linkage to Gaucher mutations in the Ashkenazi population: effect of drift on decay of linkage disequilibrium and evidence for heterozygote selection. Blood Cells Mol Dis 26:348-359, 2000

21.   Stevens J: Brightness inhibition re size of surround. Perception & psychophysics 2:189-192, 1967

22.   Pedersen JF, Larsen VA, Bytzer P, Madsen LG, Hamberg O: Hepatic transit time of ultrasound contrast in biopsy characterized liver disease. Acta radiologica 46:557-560, 2005

23.   Hoeffner EG, et al.: Cerebral perfusion CT: technique and clinical applications. Radiology 231:632-644, 2004

24.   Mettler FA, Guiberteau MJ: Essentials of nuclear medicine imaging, 2012

25.   Kim KW, et al.: Quantitative CT color mapping of the arterial enhancement fraction of the liver to detect hepatocellular carcinoma. Radiology 250:425-434, 2009

26.   Nino-Murcia M, Olcott EW, Jeffrey RB, Jr., Lamm RL, Beaulieu CF, Jain KA: Focal liver lesions: pattern-based classification scheme for enhancement at arterial phase CT. Radiology 215:746-751, 2000

27.   Khan AS, Hussain HK, Johnson TD, Weadock WJ, Pelletier SJ, Marrero JA: Value of delayed hypointensity and delayed enhancing rim in magnetic resonance imaging diagnosis of small hepatocellular carcinoma in the cirrhotic liver. J Magn Reson Imaging 32:360-366, 2010

28.   Materne R, et al.: Non-invasive quantification of liver perfusion with dynamic computed tomography and a dual-input one-compartmental model. Clin Sci (Lond) 99:517-525, 2000